JOURNAL OF MATERIALS SCIENCE **40** (2005) 1201 – 1208

Formation of porosity in ferritic ODS alloys on high temperature exposure

M. TURKER
Gazi University, Technical Education Faculty, 06500, Besevler-Ankara-Turkey
E-mail: mturker@gazi.edu.tr

In order to investigate the formation, distribution, growth behavior and volume fraction of porosity at high temperatures in ferritic Oxide Dispersion Strengthened (ODS) superalloys MA 956, ODM 751 and PM 2000 were exposed at 1100 and 1200°C in air and in 2% oxygen containing nitrogen atmospheres for up to 8760 h. All samples exhibited small amounts of porosity (% <0.1) in the as-received condition. During the early stages of exposure (up to 10 h) pores were generally located close to the surface of the samples. Later they were found in the central region of the samples and the volume fraction of porosity and the mean pore size increased. After exposure for 240–1000 h, mainly depending on sample thickness, the size and volume fraction of porosity reached a maximum value and then decreased. SEM and EDS analysis results showed that some pores contained small amounts of Ti, Al and Y rich particles which were distributed over the internal surface of pores. It was noted that when the volume fraction of porosity and the size of pores began to decrease the pores had filled with the matrix material. A relation was established between the production environment of the materials and the growth behavior of the pores.

1. Introduction

ODS alloys produced by mechanical alloying (MA) exhibit exceptional resistance to creep and oxidation, at elevated temperature [1, 2]. However, the alloys produced by powder metallurgy techniques are often characterized by the presence of significant amounts of microstructural inhomogeneties such as residual porosity and non-metallic inclusions. Such defects influence the mechanical properties of these materials. Mechanically alloyed materials contain only very small amounts of residual porosity [3, 4] and very few exogenous inclusions. However, after prolonged exposure at high temperatures these samples too showed some porosity. These defects develop very quickly at high temperatures and may shorten the useful life of these parts in a catastrophic manner [5].

Several workers [3, 6–9] have reported the formation of sub-surface porosity during oxidation, mainly in Ni based alloys. Some others [10–13] have reported the formation of internal porosity in iron based ODS superalloys. Pores in chromia forming Ni and Co based alloys are generally associated with the oxide-metal interface, whereas they are remote from the metal oxide interface in alumina forming iron based alloys.

Some debate has arisen as to whether the porosity formed during the high temperature exposure of ODS alloys in oxidizing atmospheres is environmentally induced [14], whether the coarse grain structure is the reason for the formation of porosity, or whether the porosity [15, 16] results from the coalescence of occluded gases entrapped during powder processing [10, 11, 17]. Some other investigators [5] have claimed that non- metallic particles, such as alumina, cause voids. The growth of these voids may be responsible for expanding the initial cavities although this mechanism in not clear yet.

Voids in Ni based alloys after long term exposure at high temperature are believed to be caused by the condensation of vacancies which are formed as a result of chromium fluxes away from the metal-oxide interface by the selective oxidation of chromium. Electron probe micro analysis (EPMA) indicated [3, 6] that porosity formation in exposed samples was accompanied by chromium depletion of the matrix near the oxide-metal interface.

Some investigators [5, 12, 15–18] have analyzed the formation of porosity in iron based ODS alloys at elevated temperatures and most have concluded that the porosity formed at high temperatures is not due to the Kirkendall effect, since the pores are mostly located remote from the scale-alloy interface. The oxide grows on iron-based alloys predominantly by the dominant migration of oxygen ions through the oxide grain boundaries, and the oxide reaction takes place at the oxide-metal interface. The formation of porosity in iron based alloys appears to be more complicated than that seen in nickel based alloys.

The tendency of Fe based ODS alloys to form pores during high temperature exposure is attributed by Hedrich [11] and Chen *et al.* [17] to the mechanical alloying process, which takes place in Ar atmospheres,

where incorporation of absorbed argon atoms occurs during mechanical alloying.

Bennett *et al.* [10] exposed several ODS alloys to varying temperatures up to 1400°C for times up to 200 h and observed the formation of voids within the middle third of the alloy section. The number of voids tended to decrease with temperature, while their size increased. Additionally most of the voids contained varying quantities of Ti and Al bearing oxides. Therefore these authors concluded that the formation of voids is probably due to the oxygen and/or water vapour adsorbed on the powder surface, together with the cover gas which is used during the fabrication process.

Korb [5] exposed some ODS alloys, including MA 956, and cast alloys at 1350°C for up to 200 h and observed significant growth of cavities only in coarse-grained specimens. Only materials made via the powder metallurgy route contained porosity. Contrary to this, molten, deformed and recrystallized Fe-Cr-Al did not contain any porosity at all, even when heat treated for extremely long times. The Ar content of MA 956 was found to be about 30 ppm but all the other specimens that showed porosity, did not contain any inert gas at all. The author claims that, since all the ODS alloys developed pores, Ar could not be the unique reason.

Porosity in ODS alloys causes a loss in ductility. The internal notch effect in the material at the pore edge results in high stresses as compared to the main stress applied and causes premature failure of the ODS alloys [11]. Formation of voids by vacancy ingestion during the oxidation process was found to be responsible for accelerating the creep fracture process and also hastened tensile fracture at ambient temperatures [8]. The influence of porosity on long term properties like cyclic thermal shock resistance was also found to be detrimental in MA 956. The elimination or reduction of porosity in ODS alloys will be beneficial for mechanical properties of these alloys.

The primary aims of the present investigation are to study internal porosity formation in order to improve our understanding of the behavior of ferritic ODS alloys during long term exposure at elevated temperatures. In addition simulated behavior in the exposure atmospheres similar to those encountered in close cycle gas turbines [4] containing nitrogen has also been studied and some understanding of the long term behavior of these materials has begun to emerge.

2. Material and experimental techniques

The compositions of the alloys used are given in Table I. In order to characterize the distribution and the morphologies of the pores, small sections were cut from the tubes and sheets, mounted in bakelite, ground through 1200 mesh SiC abrasive paper and finely polished down using 1 μm diamond paste. All photomicrography was performed using a Reichert MeF3 projection and Olympus microscopes.

Mounted nickel plated samples used for optical microscopy were lightly etched in Vilella's reagent for few seconds before examination in a CAMSCAN Series 4 SEM which is equipped with a windowless energy dispersive X-ray detector. Measurement of the volume fraction of porosity was made on polished sections using a simple point counting technique [18, 19].

TABLE I Composition of alloys in wt%

Alloys	Fe	Cr	Al	Ti	Mo	Y
MA 956	Bal	20	4.5	0.5	–	0.5
ODM 751	Bal	16.5	4.5	0.6	1.5	0.5
PM 2000*	Bal	20	5.5	0.5	–	0.5

*This batch of PM 2000 is reputed to have been fabricated from powder processed entirely under H_2.

2.1. Exposure testing and quantitative metallography

Exposure testing was carried out at 1100°C and 1200°C on sheet, plate and tube materials as shown in Table II. The sheets and plates were cut to form coupons with dimensions of approximately 20 × 15 mm and tubes were cut into 10–20 mm long pieces. All exposure tests in air were performed in a muffle furnace calibrated with a Pt/Pt 13% Rh thermocouple to obtain a uniform temperature zone. A maximum temperature

TABLE II Conditions used for exposure tests on samples used in the present study

Sample	Thickness (mm)	Exposure temp. (°C)	Environment	Exposure time (h)
MA 956 RX sheet	1.0			
MA 956-CR sheet	1.2	1100	Air	2.5, 24, 240, 1200, 2400, 4800, 8760
ODM 751 tube	2.4			
MA 956 sheet	1.0			
MA 956-HR	6.0			
MA 956-CR	1.2	1200	Air	1, 10, 100, 500, 1000
ODM 751 tube	2.4			
PM 2000 sheet	1.8			
ODM 751 tube	2.4	1200	Air	2.5, 24, 240, 1200, 2400, 4800, 8760
ODM 751 tube	2.4		2% Oxygen	
MA 956 RX sheet	1.0	1200	in nitrogen	2.5, 24, 240, 1200, 2400, 4800, 8760

RX: Recrystallized ; CR: Cold rolled; HR: Hot rolled.

variation of $<\pm 5^{\circ}$C was allowed within the chosen zone.

Exposure testing under controlled atmosphere conditions was performed in a closed recrystallized alumina tube furnace. Nitrogen and compressed air were mixed together in the ratio 10:1 to give an oxygen content of 2%. The gas mixture was dried before passing through the recrystallized alumina tube furnace. Temperature control in the furnace was better than $\pm 5^{\circ}$C.

Measurement of the volume fraction of porosity was made on polished and lightly etched (2–3 s) sections using a simple point counting technique. In this method, a systematically random array of points is applied to the microstructure and the number of points lying within the chosen features is counted. Then if,

$$\begin{aligned} P_{\mathrm{f}} &= \text{number of points in features and} \\ P_{\mathrm{T}} &= \text{total number of points} \\ \text{Area fraction} &= A_{\mathrm{f}} = P_{\mathrm{f}}/P_{\mathrm{T}} = \text{Volume fraction} \end{aligned} \tag{5.2}$$

An estimate of the accuracy of the measurements can be obtained using the following equation:

$$\frac{\sigma A_{\mathrm{f}}}{A_{\mathrm{f}}} = \sqrt{\frac{(1 - A_{\mathrm{f}})}{P_{\mathrm{f}}}} \tag{5.3}$$

where σ_{Af} = standard deviation

3. Experimental results

3.1. Internal porosity at 1100°C

Comprehensive and long term (up to 1 year) exposure tests at 1100°C were carried out on MA 956 recrystallized sheet, MA 956 cold rolled sheet and ODM 751 tube. In order to investigate the formation and the growth rate of porosity, lightly etched longitudinal sections of the alloys were examined using optical and scanning electron microscopes. All the as-received samples showed small amounts (<0.05%) of porosity or inclusions, generally close to the surface of the section (Fig. 1a). In the as-received condition ODM 751 tube contained the largest amount of detectable porosity, whereas MA 956 cold rolled sheet contained the least. The volume fraction and the mean size of the pores in all the samples increased with exposure time and reached a maximum then decreased. After relatively short exposure times (24 h), the porosity content increased slightly but the pores displayed a distinct tendency to concentrate in the central one third of the sample cross section. This inhomogeneous distribution became even more pronounced with increasing exposure time up to about 1200 h after which the pore content decreased. Fig. 1b to e show the growth and distribution of porosity in ODM 751 tube during exposure at 1100°C for times up to 8760 h.

Fig. 2 shows the change in total volume fraction of porosity in MA 956 recrystallized sheet, MA 956 colled rolled sheet and ODM 751 tube with exposure. Alloy MA 956 recrystallized sheet developed the largest amount of porosity after exposure whereas MA 956 cold rolled sheet fostered the lowest.

The volume fraction of porosity in MA 956 sheet increased with increasing exposure time and reached a maximum of 0.32% after exposure for 240 h with a maximum pore size of about 35 μm. Thereafter, the porosity content decreased slowly and after 8760 h the level had dropped to its low initial value.

Alloy MA 956 cold rolled sheet showed the lowest volume fraction of porosity throughout exposure. A maximum of 0.18% was attained after 1200 h and this decreased steadily to 0.02% after an exposure of 8760 h.

The ODM 751 tube followed a similar trend reaching a maximum volume fraction of 0.24% after 240 h before decreasing in a similar manner to the other alloys at a slower rate. After an exposure of 8760 h it retained the highest amount of porosity (0.12%).

Examination of the pores in the SEM revealed that they were generally rounded and contained fine Ti, Al and Y rich particles distributed over their internal surface. Titanium was the most frequently detected element. In some samples, generally those exposed for longer than 240 h, some of the pores were found to be 'filled' with material which had the same composition as the surrounding matrix.

3.2. Internal porosity at 1200°C

The most comprehensive and detailed investigations were carried out on samples exposed for times up to 8760 h at 1200°C both in air and in a reduced oxygen partial pressure. Lightly etched longitudinal sections of all the as-received materials showed small amounts (<0.1%) of fine porosity. These pores often occurred as elongated stringers close to the surfaces of the samples with the central regions appearing to be essentially pore free or containing very small amounts of porosity. It was notable that all the ODM alloys initially contained significantly higher porosity levels than MA 956 and PM 2000.

The kinetics of porosity formation during exposure at 1200°C are presented in Fig. 3. During the early stages of exposure (up to 10 h), the porosity remained fine and in the form of stringers and slowly became more homogeneously distributed. With increase in time, the volume fraction and the mean pore size increased and the pores tended to congregate in the central regions of the section. Between about 240 and 1000 h (depending on the sample thickness) the volume fraction of porosity reached a maximum value and then started to decrease. The maximum pore size at maximum volume fraction was about 50 μm.

The samples exposed at 1200°C for up to 1000 h showed higher volume fractions of porosity compared to those of samples exposed at 1100°C although the amount of porosity was found to vary considerably from sample to sample. Generally, alloy PM 2000 sheet showed the smallest porosity content throughout the exposures whereas ODM 751 tube showed the highest. After exposure for 500 h, the porosity

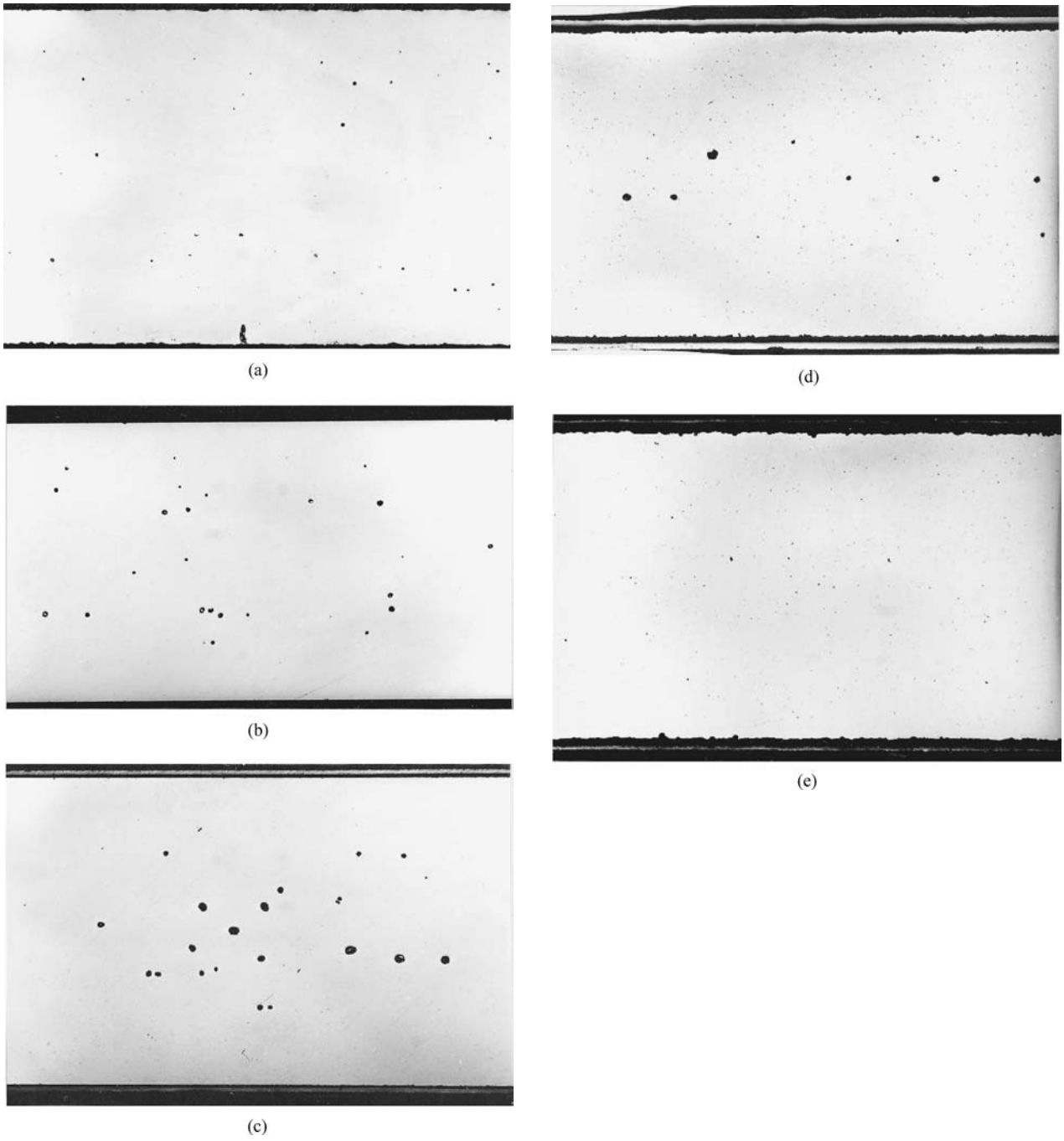

Figure 1 (a–e) Changes in size and distribution of internal porosity in ODM 751 tube during exposure in air at 1100°C. (a) As received, (b), 24 h, (c) 240 h, (d) 2400 h, and (e) 4800 h.

content in all samples, except MA 956 cold rolled sheet, reached a maximum value and then started to decrease slightly.

Since some decrease in the volume fraction of porosity was noted in most of the alloys after 500 or 1000 h exposure, it was believed that longer exposure times gave a better indication of the kinetics of pore growth. The volume fraction of porosity was measured on samples of MA 956 recrystallized sheet and ODM 751 tube exposed in 2% oxygen and also on ODM 751 tube exposed in air for up to 8760 h (1 year) and the results are presented in Fig. 4.

All samples showed a very similar porosity content in the early stages of exposure. However, the thinner MA 956 recrystallized sheet showed a slightly higher volume fraction of porosity up to 240 h when it reached a maximum value of 0.42% and then started to decrease. On the other hand both ODM 751 tubes, exposed in either air or 2% oxygen showed an increase in porosity content up to 1200 h and reached maximum values of 0.51% and 0.41% respectively. Further exposure resulted in a decrease in the porosity content in both samples. At the end of 8760 h, the volume fraction of porosity measured in ODM 751 exposed in air was 0.18%, whereas it was 0.32% for the ODM 751 sample exposed in 2% oxygen.

3.3. Effect of sample thickness on porosity

In order to examine the effect of the section thickness on the amount and distribution of porosity, a series of experiments was performed using MA 956 recrystallized

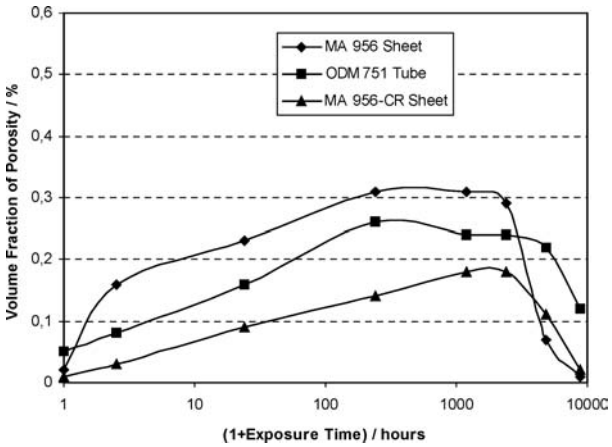

Figure 2 Effect of exposure time at 1100°C in air on porosity content of MA 956 and ODM 751.

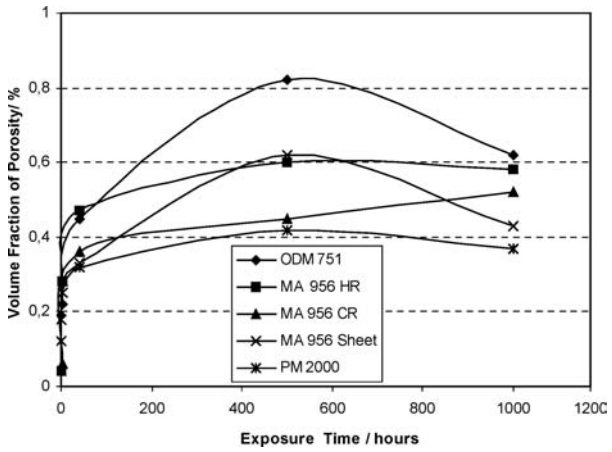

Figure 3 Effect of exposure time at 1200°C on total porosity content of ODS superalloys.

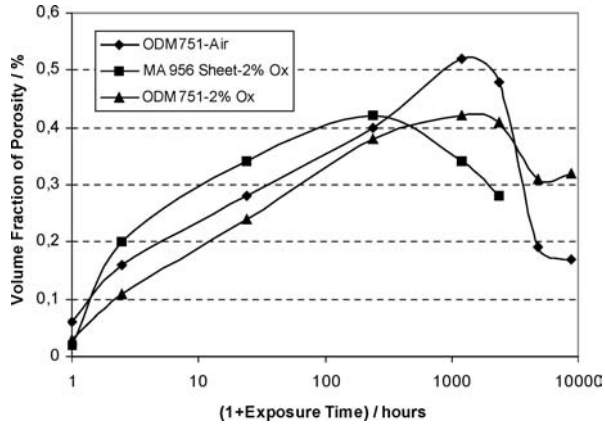

Figure 4 Effect of exposure time and atmospheres at 1200°C on total porosity content.

sheet, MA 956-cold rolled sheet and ODM 751 tube. Sheet samples were ground down to 0.5 mm and the outer surface of the ODM 751 tube was machined down to reduce its wall thickness from 2.4 mm to 1.1 mm. Both normal and thinned samples were then exposed together for 1200 h at 1200°C and the volume fraction of porosity measured. The results are given in Table III and the micrographs of the sections are shown in Fig. 5. It was found that the volume fraction of porosity was strongly dependent on the sample thickness and thinner samples contained a considerably smaller amount of porosity than thicker samples after the same exposure times.

TABLE II Volume fraction of porosity in as-received and thickness reduced samples after exposure at 1200°C for 1200 h

Sample	Thickness (mm)	V_f (pores) (%)
MA 956 RX sheet	1.0	0.90
MA 956 RX sheet	0.5	0.05
MA 956-CR sheet	1.25	0.57
MA 956-CR sheet	0.5	0.17
ODM 751 tube	2.4	0.60
ODM 751 tube	1.1	0.16

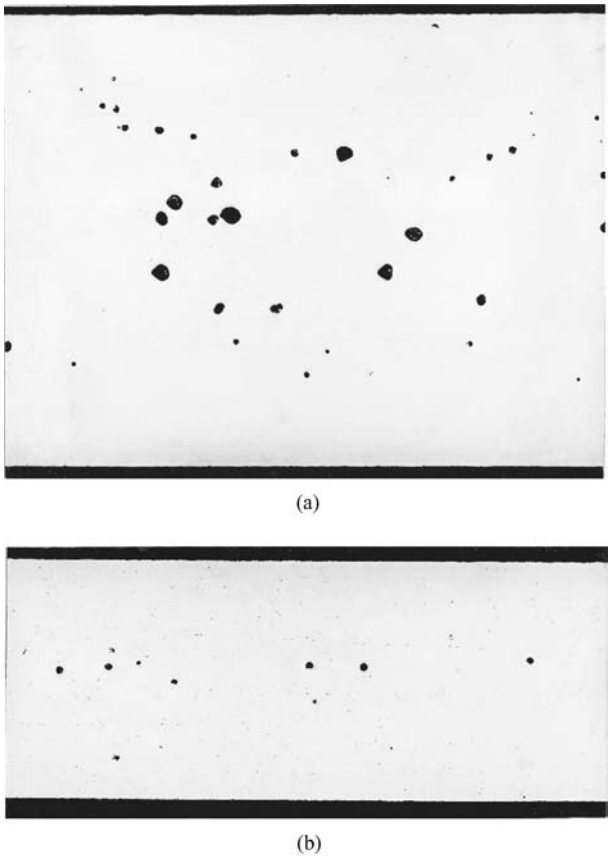

Figure 5 Effect of sample thickness on porosity content of ODM 751 tube exposed for 1200 h at 1200°C. (a) wall thickness = 2.4 mm, (b) wall thickness = 1.1 mm.

3.4. Characterization of porosity

Analysis of the pores using an analytical SEM revealed that they were generally spherical (Fig. 6) and contained some Ti rich particles at the pore-matrix interface. Some pores contained a few Ti, Al and Y containing particles and these were generally distributed over their internal surface. Fig. 7 shows the distribution of pores on the fracture section of the ODM 751 tube after exposure for 500 h.

It was noted that the number and the size of the pores began to decrease and the pores became irregular in shape for exposures longer than 240 h (Fig. 8). This is attributed to the 'filling' of pores by the matrix material. The original surfaces of the pores could be identified as they were clearly delineated by second phase particles.

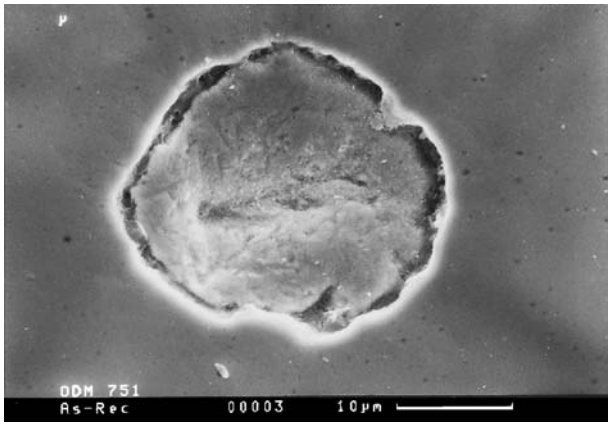

Figure 6 SEM micrograph showing porosity present in as-received ODM 751 tube.

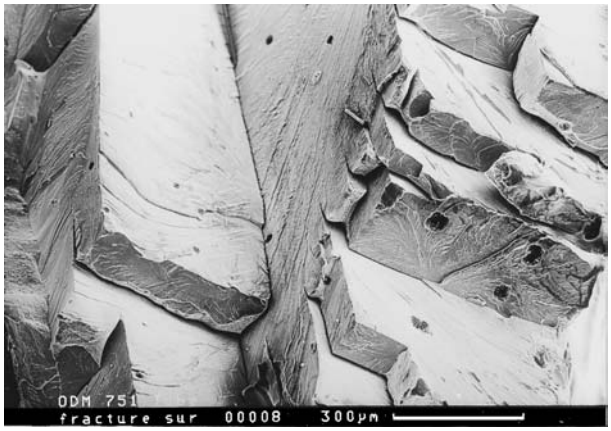

Figure 7 SEM micrograph showing the distribution of pores on a brittle fracture surface of ODM 751 tube exposed for 500 h at 1200°C.

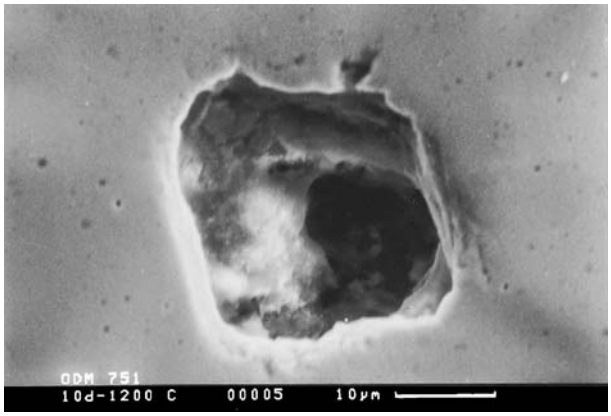

Figure 8 Irregularly shaped pore formed in ODM 751 tube after exposure for 240 h at 1200°C.

These particles remained even after the pores had become completely 'filled' by matrix. Fig. 9 shows the partially filled pores seen in the MA 956 sheet after an exposure for 1200 h at 1200°C. However, very few pores did not shrink in diameter after very long exposure times.

In order to analyze the relation between defects (such as coarse second phase particles, inclusions or unrecrystallized areas) and the formation of porosity in both as-received and exposed ODM 751 tubes, samples were carefully polished using colloidal silica to obtain a very

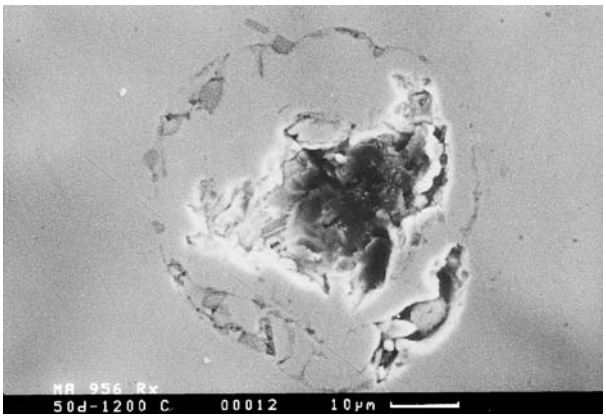

Figure 9 SEM micrographs showing partially 'filled' pore in MA 956 sheet after exposure for 1200 h at 1200°C.

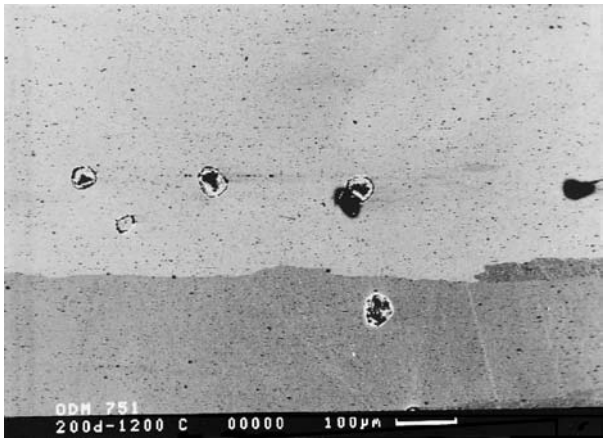

Figure 10 Backscattered electron image showing an array of partially 'filled' pores which are not associated with boundaries or other defects in ODM 751 tube exposed 4800 h at 1200°C.

fine surface finish and later analyzed using the backscattered imaging mode in a SEM and a very low working distance (7 mm) to show grain orientation without etching.

Although a few very small grains were found near pores in some regions, in general, no relation was found between defects and porosity. Some pores found to be formed near small grains in the as-received ODM 751 tube. However, most were remote from grain boundaries in ODM 751 tube exposed for 4800 h (Fig. 10).

4. Discussion

The formation of internal porosity was observed in all alloys during prolonged high temperature exposure. Some authors [3] claim that these pores are derived from the condensation of Kirkendall vacancies created by the outward flux of atoms in the matrix to form protective oxide layer at the surface. This has been observed in chromia forming Ni based alloys in which most of the pores are located near the metal/oxide interface where most chromium depletion occurs. However, the mechanism of pore formation in alumina forming Fe based alloys is still unclear since alumina grows inward and the Al depletion is uniform throughout the sample section [18, 19]. If pores are formed due to Kirkendall vacancies, the volume fraction of voids should increase

monotonically with time as the surface scale thickens provided that the vacancy annihilation rate is significantly less than the condensation rate of a decreasing vacancy flux. The volume fraction should also depend on the section thickness; after a given exposure time there should be a larger volume fraction of voids in thinner sections than in thick sections of the same surface area.

If, on the other hand, the voidage is due to the precipitation of slow moving gas atoms [10, 11], then the outer regions should contain relatively little porosity since the scale/metal interface should act as an effective sink. In addition, one would expect the total volume fraction to initially increase with time and then decrease as more and more diffusing gas is lost to the surface, so that eventually all the voidage is eliminated. Furthermore, the volume fraction should be smaller in thinner sections since gas atoms can dissolve in the matrix and diffuse to the surface more rapidly than in thicker sections. However, since the excess pressure in large gas filled pores is very small, the solubility in the matrix will also be small so that coarsening and dissolution rates must be very low.

The present results reveal that the volume fraction of porosity is strongly dependent on sample thickness. In a sample of 1 mm thick MA 956 sheet (Fig. 4) the volume fraction reaches a maximum of 0.44 wt% after 240 h exposure at 1200°C and then starts to decrease. On the other hand, the volume fraction only reaches a maximum of about 0.55 wt% after 1200 h in the 2.4 mm thick ODM 751 tube in the same exposure test. The effect of sample thickness on the porosity content was clearly demonstrated (Fig. 5 and Table III) when the as-received and the thickness-reduced samples of MA 956 recrystallized sheets and ODM 751 tubes were exposed together for 1200 h at 1200°C. All the thin samples showed a considerably lower volume fraction of porosity ($<$0.18 wt%) compared to the thicker samples ($>$0.60 wt%). Since the metal /oxide interface may act as a sink for vacancies, gas atoms from the pores in the thinner samples can reach the surface more easily and result in a decrease in the amount of porosity.

In the early stages of exposure, the pores are fine and in the form of stringers and appear to be fairly homogeneously distributed. As the exposure time increases, the mean pore size increases and the number decreases consistent with an Ostwald ripening process. Most of the coarse voids occur in regions remote from the free surfaces and most tend to congregate in the central part of the section as a consequence of the edge effects [18, 19]. Under most circumstances, the total volume fraction of porosity reaches a maximum and then slowly decreases. Both of these observations lend substantial support to the entrapped gas mechanism which has been previously reported by others [10, 11, 19].

After exposures of longer than 240 h (and again dependent on sample thickness) some coarse pores were found to have filled with matrix material although their original surfaces remained delineated by rings of small second phase particles. When the porosity content within the matrix reaches a maximum further exposure results in the dissolution of gas from the pore surface into the matrix which then diffuses to the metal/oxide interface and effectively disappears.

It has also been claimed [5] that the formation of porosity is in some way related to the presence of coarse second phase particles within the matrix. There is a little information on the influence of non-metallic particles on the formation of porosity. The present results reveal that many but not all pores contained second phase particles distributed over the inner surface. Also the second phase particles in the bulk of the alloys were not generally associated with pores. It is also reported that [20] yttria particles are not responsible for the initiation or the formation of porosity, since yttria-free ferritic alloys also exhibit porosity. Furthermore, when MA alloys were melted down and reforged into bar stock, the porosity problem disappears. It must therefore be concluded that the role of second phase particles in pore formation is dubious with little direct evidence to support the suggestions of Korb [5].

Alloy PM 2000 exhibited the smallest amount of porosity amongst the alloys exposed at 1200°C in air. This sample was reputed to have been milled under hydrogen gas rather than argon during the long mechanical alloying process. Since the diffusivity of hydrogen is many order of magnitude faster than argon in ferrite, hydrogen can diffuse from the powder easily during subsequent processing. If the mechanism of pore formation is associated with entrapped gas then in PM 2000 the amount of porosity should be very low. Measurements showed that in the hydrogen-processed alloy the maximum amount of porosity was much lower (Fig. 3) than those processed conventionally under argon gas.

5. Conclusions

In order to investigate the formation, distribution and the growth behavior of porosity at high temperatures, ferritic ODS alloys were exposed at 1100 and 1200°C in air and in 2% oxygen containing nitrogen atmospheres for up to 8760 h. All samples contained small amounts of porosity in their as-received condition and in the early stages of oxidation. The size and volume fraction of pores slowly increased with time and they become preferentially located in the central one-third of the sample. After a finite time, dependent on sample thickness, the volume fraction reached a maximum and then decreased gradually. These observations are consistent with an entrapped gas mechanism. PM 2000, processed in hydrogen rather than argon, developed significantly less porosity than all other alloys. This result also suggests that the internal voidage is mainly associated with condensation of gas occluded into the material during processing.

References

1. M. TURKER, *Corros. Sci.* **4-1/1** (1999) 1.
2. M. TURKER, H. CAMA and T. A. HUGHES, *Corros. Sci.* **37** (1995) 413.
3. A. H. ROSENSTEIN, J. K. TIEN and W. D. NIX, *Met. Trans.* **17A** (1986) 151.

4. M. TURKER and T. A. HUGHES, in Proceedings of the 2nd International Conference on Microscopy of Oxidation (Cambridge, March 1993) p. 301.
5. G. KORB, in Proceedings of Conference on New Materials by MA Techniques, edited by E. Artz and L. Schultz (Calw-Hirasu, 1989) p. 175.
6. J. H. WEBER and P. S. GILMAN, *Scripta Metallurgia* **18** (1984) 479.
7. J. J. STHEPENS and W. D. NIX, *Met. Trans.* **16A** (1985) 1307.
8. P. HANCOCK, in Proceedings of Conference on Vacancies'76, Bristol, edited by R. E. Smallman and J. E. Harris (Bristol University Met. Soc., 1976) p. 215.
9. J. KOMENDA and P. J. HENDERSON, *Scripta Materialia* **37** (1997) 1821.
10. M. J. BENNETT, H. ROMARY and J. B. PRICE, in Proceedings of Conference on Heat Resistance Materials (Fortana, Wisconsin, September 1991) p. 95.
11. H. D. HENDRICH, in Proceedings of Conference on New Materials by MA Techniques, edited by E. Artz and L. Schultz (Calw-Hirasu, 1988) p. 217.
12. M. TURKER and T. A. HUGHES, *Oxidation of Metals* **44** (1995) 505.
13. J. RITHERDON and A. R. JONES, *Mat. at High Tem* **18** (2001) 177.
14. H. D. HENDRICK, in "High Temperature Materials for Power Engineering" Part 1 (1990) p. 789.
15. Y. L. CHEN and A. R. JONES, *Met. Mater. Trans. A* **32A** (2001) 2077.
16. P. K. SUNG, D. R. POIRIER, S. D. FELICELLI, E. J. POIRIER and A. AHMED, *J. Crystal Growth* **226** (2001) 363.
17. Y. L. CHEN, A. R. JONES and U. MILLER, *Met. Mater. Trans. A* **32A** (2002) 2713.
18. M. TURKER, in Ph.D Thesis, University of Leeds School of Materials, UK, 1993.
19. M. TURKER, "8th International Metallurgy and Materials Congress" (Istanbul, Turkey, 1995) p. 161.
20. F. STARR, Private Communication (British Gas London Research Station).

Received 29 December 2003
and accepted 7 October 2004